COLLEGE OF ENGINEERING
DEPARTMENT OF CIVIL ENGINEERING (CVEG)
STEEL STRUCTURES RESEARCH LABORATORY (SSRL)

SSRL Report N° 2019/1

# Investigation into Shear Stud Fatigue Demands

*Towards Modification of the Existing AASHTO Stud Fatigue Provisions*

**Brian Hillhouse**
**Gary S. Prinz, Ph.D., P.E.**

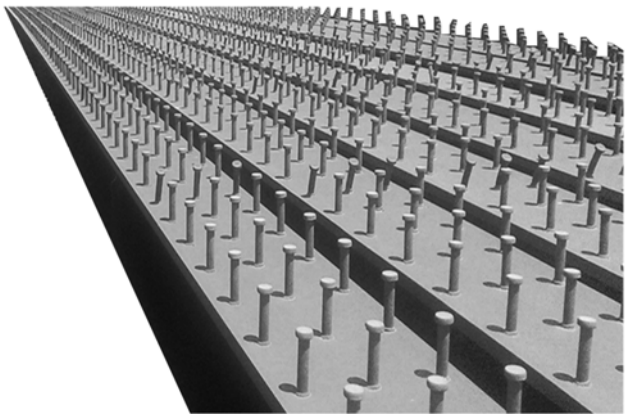

SSRL Project N° 0402 63768-21-0000
Final report submitted to the American Institute of Steel Construction (AISC)

March, 2019

COLLEGE OF ENGINEERING
DEPARTMENT OF CIVIL ENGINEERING (CVEG)
STEEL STRUCTURES RESEARCH LABORATORY (SSRL)

University of Arkansas
Department of Civil Engineering
4190 Bell Engineering Center
Fayetteville, AR 72701

Telephone : + 1 (479) 575-2494
Fax : + 1 (479) 575-7168
E-mail : prinz@uark.edu
Website : www.ssrl-uark.com


**V/ref :** **Fayetteville, AR, March 2019**
**N/ref : CVEG** **Report SSRL N° 2019/1**

# Investigation into Shear Stud Fatigue Demands

*Towards Modification of the Existing AASHTO Stud Fatigue Provisions*

| | |
|---|---|
| **Mandate:** | American Institute of Steel Construction (AISC) |
| **Mandate Description:** | Experimental investigation into the effects of stud clustering and flange surface friction on measured stud shear demands during fatigue loading. |
| **Date of Mandate:** | Anticipated start date: May 1, 2018<br>Project funds received: July 24, 2018 |
| **Specimens:** | 4 full-scale composite girders having varied stud configurations. |
| **Reception of the Specimens:** | June 2018 |
| **Testing Dates:** | June 2018 – March 2019 |
| **Project PI:** | G.S. Prinz |
| **Report Authors:** | B. Hillhouse and G.S. Prinz |

**Signatures :**

Project PI

Gary S. Prinz, PhD, PE

This report contains 28 pages (plus 10 pages of front matter)

## ACKNOWLEDGEMENTS

This report presents the results of a research project sponsored by the American Institute of Steel Construction. We acknowledge the financial support provided by AISC as well as the assistance and encouragement of the project lead, Mr. Tom Schlafly. Expert advice provided throughout the project by Dr. Justin Ocel (FHWA Office of Infrastructure Research and Development) and Dr. Cameron Murray is also recognized. The research was conducted in the Steel Structures Research Laboratory (SSRL) at the University of Arkansas. Laboratory staff and graduate students instrumental in the completion of this work include: David Peachee, Gabriel Cook, and Caleb LeBow. Additional insight and guidance on the research project was provided by the Bridge Task Force Design Advisory Group consisting of experts in the field of bridge engineering. Although many individuals contributed to the research findings presented herein, the authors accept full responsibility for the conclusions presented.

*(Page Intentionally Left Blank)*

## EXECUTIVE SUMMARY

This report presents a novel approach to measuring shear stresses within embedded studs and investigates the effects of stud clustering and steel flange surface friction on resulting stud demands during fatigue loading. In this study, thin, flexible pressure-gauges are attached to the studs of composite beam specimens to measure the peak contact pressure and allow calculation of stud shear demands from existing elasticity theory. A total of three large-scale composite girders are fatigue tested, representing both uniform and clustered stud configurations and two levels of flange surface friction. One non-composite beam test is also performed to better understand friction contributions to composite action. Results from the fatigue testing and instrumentation suggest that stud demands estimated by the AASHTO provisions are conservative. All composite specimens survived over 4,500,000 fatigue cycles at an applied stress range of 67.6MPa (9.8ksi) while maintaining full composite action and experiencing negligible increases in slab slip. Stud shear stress measurements for specimens having a Class A flange friction surface (cleaned mill scale surface) experienced stud demands that were nearly 66% lower than those estimated by the AASHTO provisions which neglect friction effects. When PTFE sheeting was added to reduce friction at the steel-concrete interface, AASHTO stud demand estimations were within 10% of measurements. Comparing stud pressure measurements between the specimens having uniform studs and clustered studs indicates higher demands within the exterior rows of clustered studs, confirming the findings in previous research by Ovuoba and Prinz (2018) [2]. A modification to equation 6.10.10.1.2-3 in the AASHTO provisions for estimating stud demands is proposed as $V_{fat} = {\mu V_f Q}/{I}$, where $\mu$ equals 0.5 for a Class A or better flange friction surface and $\mu$ equals 1 for all other flange friction conditions.

***Research Implementation:*** Based on the results of the current project and other recent works by the author (G.S. Prinz) and the Federal Highway Administration (FHWA), an NSBA Technical Committee has been initiated to propose revisions to the shear stud LRFD design provisions. It is anticipated that the task group (which includes PI Prinz) will present a ballot item implementing the abovementioned findings, to be voted on by the AASHTO T-14 Committee on Structural Steel Design.

***Research Products:*** Following are the scientific publications resulting/pending from the AISC shear stud research project.

- Hillhouse, B., and **Prinz, G.S.** (2019). "Effects of clustering and flange surface friction on headed shear stud demands." *Journal of Bridge Engineering*, [Under Review]

***Ongoing Work:*** With the help of industry partners at W&W|AFCO Steel we have identified three existing high-traffic bridges for stud magnetic particle and die penetrant inspection (following deck removal). These bridges to be inspected include: 1) a bridge widening in Little Rock, Arkansas, along Interstate 630 (constructed in the late 1970's), 2) deck removal on a bridge along Interstate 30 south of Benton (constructed in the early 1960's), and 3) a bridge over the White River along Interstate 40 (constructed in the 1960's). Due to construction schedules, access for fatigue crack inspections were not possible during the

project timeline. These inspections are to be carried out sometime in 2020 and will be documented in a report addendum. Note that two stud fatigue-crack inspections on existing highway bridges have already been completed and are documented in the journal publication listed below.

- Ovuoba, B., and **Prinz, G.S.** (2018). "Investigation of residual fatigue life in shear studs of existing composite bridge girders following decades of traffic loading." Engineering Structures, 161 (2018), pp.134-145.

## TABLE OF CONTENTS

*(Page Intentionally Left Blank)*

## LIST OF FIGURES

*(Page Intentionally Left Blank)*

## LIST OF TABLES

*(Page Intentionally Left Blank)*

## NOTATION

The following terms are used in the text of this report:

| | | |
|---|---|---|
| *AASHTO* | = | American Association of State Highway Transportation Officials; |
| $D$ | = | stud diameter; |
| $f'_c$ | = | concrete compressive strength; |
| $F_R$ | = | total applied force on embedded stud from surrounding concrete; |
| $I$ | = | composite section moment of inertia; |
| $L$ | = | stud pressure distribution length; |
| $n$ | = | number of transverse studs on beam top flange; |
| $p$ | = | stud pitch (longitudinal spacing); |
| $P_{max}$ | = | peak applied pressure; |
| *PTFE* | = | polytetrafluoroethylene; |
| $Q$ | = | first area moment of composite section; |
| $V_{sr}$ | = | shear flow at steel-concrete interface; |
| $Z_r$ | = | stud fatigue capacity; |
| $\Delta P$ | = | change in pressure; |
| $\Delta R$ | = | change in resistance; |
| $\Delta\tau$ | = | shear stress range; |
| $\Omega$ | = | resistance, ohms; |
| $\theta$ | = | stud surface location angle; |
| $\mu$ | = | Proposed fatigue demand flange surface friction correction factor (0.5 for Class A or better surface, 1.0 otherwise) |

*(Page Intentionally Left Blank)*

**RESEARCH REPORT**

## 1. Introduction & Background

Recent analytical research suggests that the current American Association of State Highway Transportation Officials (AASHTO) LRFD Bridge Specifications [1] underestimate stud fatigue demands for clustered stud groupings spaced greater than 24 inches (0.61m) [2]. Other research suggests that AASHTO predictions overestimate stud fatigue demands for more uniformly spaced stud configurations [3-8]. Whether current code provisions over or underestimate actual stud demands for different stud configurations, these research findings have not been directly confirmed with experimental measurement due to the difficulties in measuring embedded stud shear demands during service-level fatigue loading.

Measuring shear stresses transferred through headed studs in composite steel-concrete members is challenging. In composite beams, studs are encased within concrete and traditional surface instrumentation techniques (i.e. strain gauges, displacement transducers, etc.) are incapable of determining resulting stud shear demands during service-type loadings. Often these surface instrumentation techniques are used to simply infer stud fatigue cracking (through reduced stud surface strains) and estimate loss of composite action from flange strains or more global measurements of slip or separation between the concrete and steel sections [5, 6, 9-12]. To understand actual stud demands during in-service fatigue loading, methods for directly measuring force transfer between the concrete and steel sections are needed.

This report presents a novel approach to measuring shear stresses within embedded studs and investigates the effects of stud clustering and steel flange surface friction on resulting stud demands during fatigue loading. The report begins by describing the stud shear stress measurement approach and then applies it to investigate demands on both uniform and clustered stud configurations in large-scale composite beam fatigue tests. Following, modifications to the current AASHTO stud fatigue demand provisions are proposed.

## 2. Shear Stud Stress Measurement Approach

Elasticity equations relating pressure distributions on embedded objects are used in this study to understand stud shear demands. The closed form solution for the resulting pressure distribution on an embedded rigid cylinder having a negligible tolerance with the surrounding material (similar to that of a stud embedded in concrete) takes the form of a cosinusoidal relationship dependent on the peak applied pressure ($P_{max}$) and cylinder surface location angle ($\theta$) (see Figure 1) [13, 14]. By integrating the horizontal components of this pressure distribution over the contact surface area (see again Figure 1), a total applied force ($F_R$) given by Equation 1 can be determined; where $L$ is the height of the pressure distribution on the cylinder, $P_{max}$ is the peak applied pressure, and $D$ is the cylinder diameter.

$$F_R = P_{max}(\pi LD)/4 \qquad \text{(Eq 1)}$$

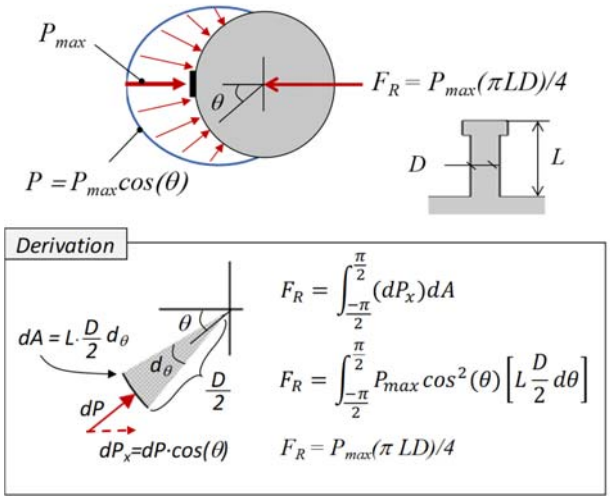


Figure 1. Pressure distribution on embedded cylinder and derivation for the resultant horizontal force.

Conditions for the above-described embedded cylinder are similar to those experienced by shear studs encased in concrete, as the primary force transfer between the concrete and steel components in a composite girder is achieved from the concrete bearing on the steel stud surface. As concrete is cast around studs, a negligible tolerance exists between the concrete and steel surfaces. Resulting stud pressure distributions due to longitudinal shear flow at the steel concrete interface would be expected to follow the same cosinusoidal relationship as shown in Figure 1. By measuring the peak contact pressure at the stud centerline along the longitudinal beam axis, the entire resultant force on the embedded stud could be determined.

In this study, thin flexible transverse pressure gauges (type PMS40 produced by HBM, inc.) are attached to the stud surface to measure the peak contact pressure and allow calculation of stud shear demands. The PMS40 pressure gauges are calibrated to relate changes in resistance to changes in pressure, similar in functionality to a strain gauge. Calibrated for high pressure applications up to 145ksi (10 kbar) the electrical output signal (measured as a change in resistance, ΔR) is related to changes in pressure (ΔP) according to Equation 2. Application of the pressure gauges to the stud steel surface is described later in Section 3.2 *Specimen Instrumentation*.

$$\frac{\Delta R}{120\Omega} = 2.5\left(\frac{10^{-6}}{bar}\right) * \Delta P \qquad \text{(Eq 2)}$$

## 3. Experimental Investigation into Stud Demands

To improve understanding of stud demands in composite beams, four large-scale composite girders were constructed, instrumented with the new pressure gauge approach (as well as traditional instrumentation approaches) and fatigue tested. The four specimens include three composite sections having both uniform and clustered shear stud configurations and one non-composite beam where the slab was merely cast on the steel beam top-flange. The non-composite beam specimen was added to the experimental matrix to better understand the extent of the friction and adhesion contributions to composite action. The three composite beam specimens were designed to have the same composite strength based on strength limit state requirements for full composite action (although stud configurations and steel surface

friction values were varied). Table 1 provides the specimen test matrix and describes the shear connector configurations and flange surface friction values considered. Calculations for determining the required stud spacing in Specimen 1, based on the AASHTO strength limit state, are given in Appendix A.

Table 1. Experimental Matrix and Specimen Descriptions

| Test ID | Test Description | Stud Spacing, in. (m) | Flange Friction Surface | Applied Force Range, kips (kN) | Average Slab Concrete Compressive Strength*** ksi (MPa) |
|---|---|---|---|---|---|
| Specimen 1 | Full composite with uniform stud spacing | 10.8 (0.27) | Class A* | 30 (133) | 6.73 (46.4) |
| Specimen 2 | Non-Composite | None | Class A | 30 (133) | 7.27 (50.1) |
| Specimen 3 | Full composite with 4 rows of clustered studs | Clusters at 51 (1.30) | Class A | 30 (133) | 7.40 (51.0) |
| Specimen 4 | Full composite with 4 rows of clustered studs | Clusters at 51 (1.30) | PTFE** | 30 (133) | 8.71 (60.0) |

* Cleaned mill scale flange surface; coefficient of static friction, $\mu$ = 0.3-0.33
** Two layers of 1mm thick PTFE sheeting between flange and slab; coefficient of static friction, $\mu$ = 0.04
*** All compressive strength measurements taken at time of fatigue testing, with cure times varying beyond 28 days

### 3.1. *Specimen Fabrication and Experimental Setup*

Figure 2 shows the typical geometry and fabrication detailing for all four beam specimens. Each specimen consisted of a rolled W18x40 section with a 6 inch thick by 18 inch-wide (152mm-thick by 457mm-wide) cast-in-place concrete slab. All composite specimens were 14 feet (4.27m) in length while the non-composite specimen was 11 feet (3.35m) in length. The chosen geometry and beam lengths are primarily based on lab testing restrictions. All shear connectors for the composite specimens were ¾ inch (19mm) diameter headed shear studs.

For the composite test specimens, two studs were placed transversely across the beam flange in both the clustered and uniform stud configurations. Figure 3 shows the different stud configurations considered. Note that the clustered shear stud configuration have the same number of total shear studs as the uniform configuration (providing the same composite shear strength).

The concrete mixture was designed using a standard highway bridge deck mix design (assuming $f'_c$ = 3.5 ksi (24MPa)) with normal weight concrete [15]. Rebar (#3 bar) spaced as shown in Figure 2 provided the minimum reinforcement requirements. Concrete cover and deck penetration for the shear studs were provided in accordance with the AASHTO provisions [1]; however, no concrete haunch was considered in the test specimen deck geometry. To simulate actual cast-in-place field conditions, the concrete of Specimens 1, 2, and 3 was cast directly onto the steel top flange (having a cleaned mill scale Class A friction surface). For Specimen 4, two sheets of 1mm thick Polytetrafluoroethylene (PTFE) were placed on the beam top-flange prior to concrete casting to reduce any flange surface friction and adhesion effects on the clustered stud configurations. For all specimens, the concrete was cast with the beam in the standard vertical position and cured outdoors (see Figure 4). To ensure adequate compressive strength (at least 80% $f'_c$), concrete cylinders were created from

the slab mix on the day of casting and evaluated at the start of each fatigue test. Table 1 shows the concrete compressive strength values on the day of testing for each specimen.

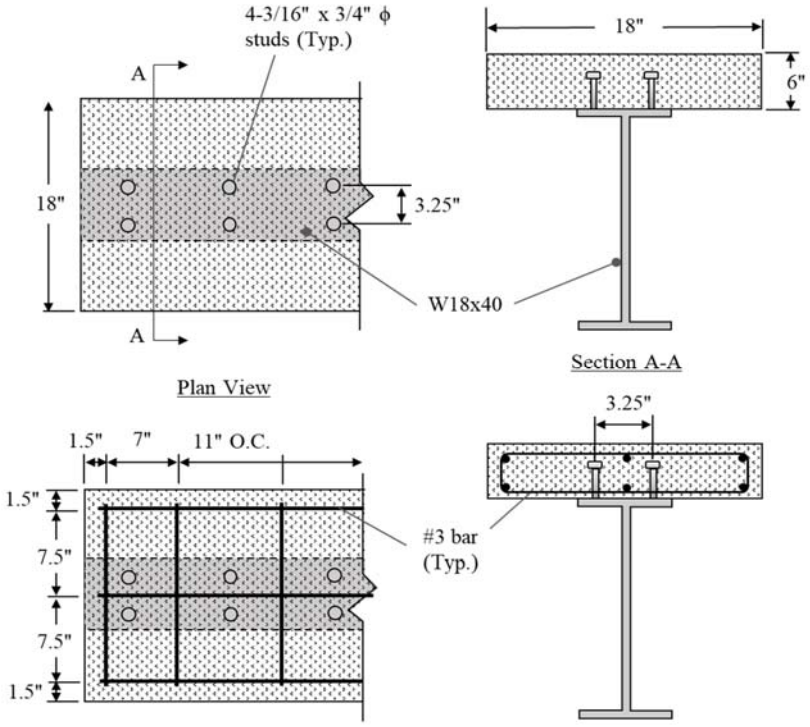


Figure 2. Geometry and fabrication detailing for the fatigue test specimens (figures not drawn to scale)

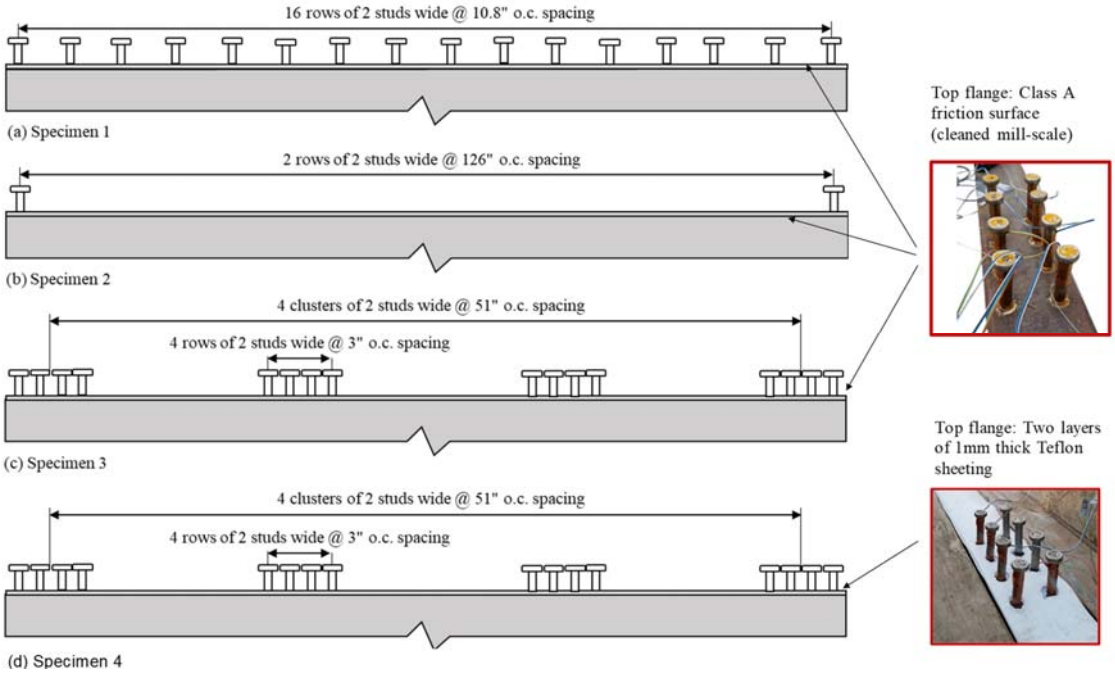


Figure 3. Stud configurations for the fatigue test specimens (figures not drawn to scale)

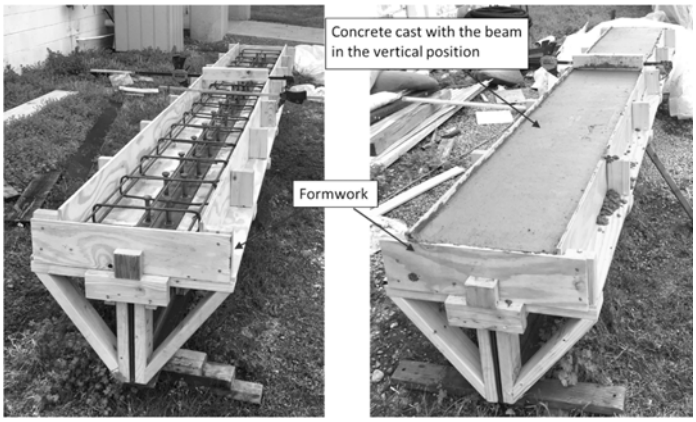


Figure 4. Specimen formwork and concrete deck casting

The experimental setup, shown in Figure 5, was designed to apply cycles of uniform shear stress to the composite beam specimens. A servo-hydraulic actuator having 110-kip (489 kN) axial compressive capacity loaded each specimen in 3-point bending; however, due to testing restrictions, the beam specimen was rotated from a typical vertical position to horizontal for testing (see again Figure 5). Blocking was placed under the beam web to ensure the beam remained parallel to the applied load during testing and PTFE pads were placed beneath the concrete portion of the beam at each end to limit friction-force transfer through the ground. An elastomeric bridge bearing-pad between the actuator and beam specimens dispersed the concentrated actuator force.

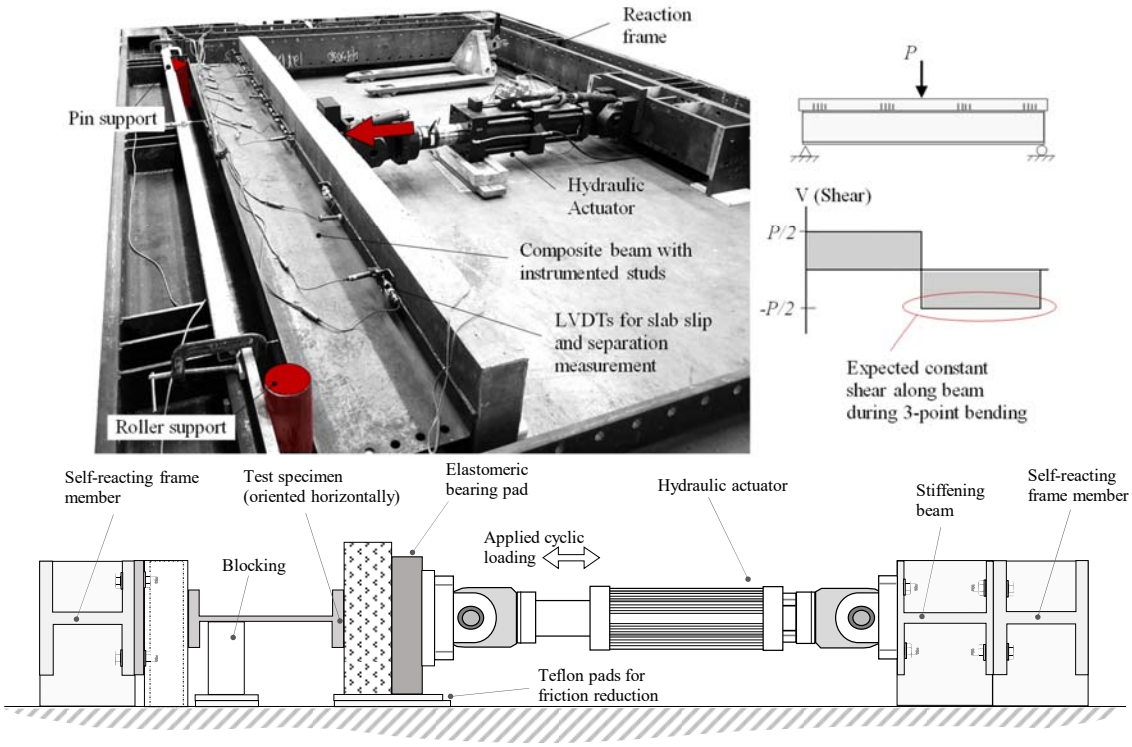


Figure 5. Simply-supported composite beam loaded in 3-point bending to produce constant shear demand between stud clusters (figures not drawn to scale).

### 3.2. *Specimen Instrumentation*

Thin foil transverse pressure gauges (type PMS40 produced by HBM, inc.) were used in this study to measure the peak contact pressure between the stud steel surface and concrete slab. Figure 6 shows the configuration of pressure gauges on the studs of Specimens 1, 3, and 4. As a reminder, Specimen 2 was constructed as non-composite with no headed shear studs and therefore no pressure gauges were provided. Also note that for Specimen 3, two shear studs had multiple pressure gauges configured along the height of certain studs to determine the vertical shear distribution needed for pressure integration across the contact surface area. As shown in Figure 6, polyimide tape was used to protect the pressure gauge electrical connections and prevent moisture damage during concrete casting.

In addition to stud pressure gauges, multiple linear variable differential transducers (LVDTs) were used to measure the relative slip and separation between the concrete deck and steel top flange. Horizontal LVDTs measured the slip along the length of the beam and the vertical LVDTs measured the separation. Slip data is used to infer shear stud damage and ultimately loss of composite action. Based on the number of available LVDTs and data acquisition channels, placement of the LVDTs was chosen to be asymmetric across the beam centerline. This provided a dense array of measurements on one half of the composite beam and a coarse array of measurements on the other half. Each specimen was also instrumented with an LVDT connected to the steel frame at the beam mid-span to measure the maximum beam deflections.

Strain gauges attached to the bottom and top-flange at the beam centerline were used to measure local steel strains during loading and allow calculation of the section neutral axis . Figure 7 shows the typical LVDT and strain gauge instrumentation configurations.

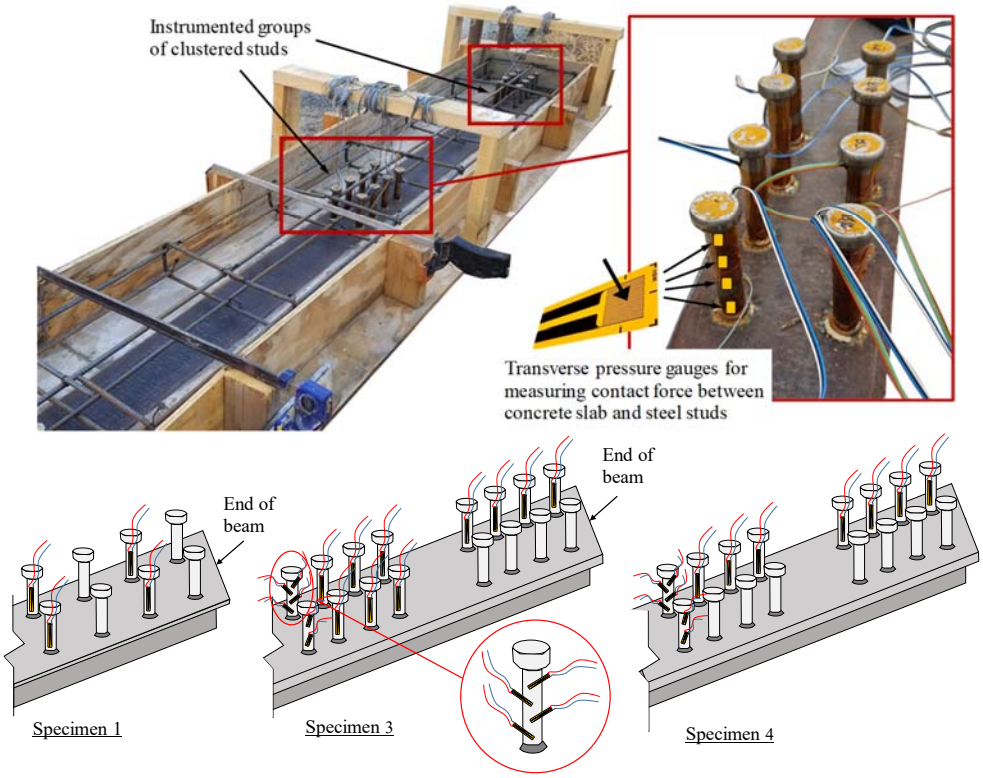


Figure 6. HBM PMS-40 transverse pressure gauge instrumentation for the three composite specimen configurations (figures not drawn to scale).

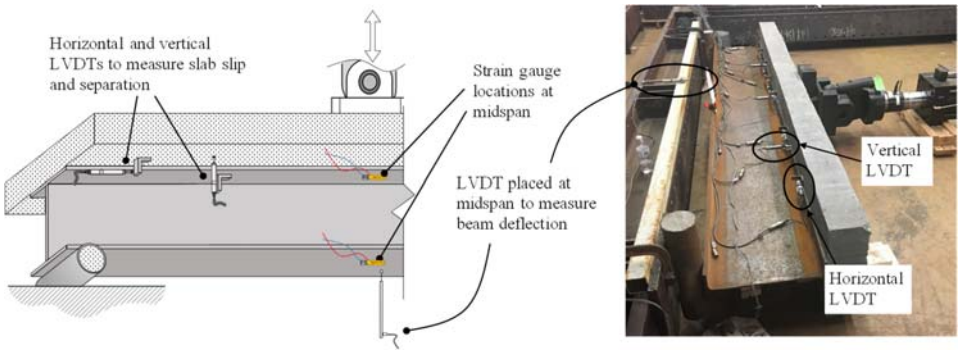


Figure 7. Local strain and displacement instrumentation (figure not drawn to scale)

### 3.3. *Specimen Loading*

Each beam specimen was subjected to repeated force cycles to simulate fatigue loading. The applied actuator force ranged from 3 to 33 kips (13.3 to 147 kN) at a loading rate of 2 Hz. Note that at least 3 kips (13.3 kN) of force was provided to prevent lift-off and subsequent pounding of the hydraulic actuator against the test specimens. The applied force range was chosen to be slightly more severe than the fatigue design truck in AASHTO [1] to accelerate fatigue damage. while remaining within the elastic range of the composite section. The service load fatigue truck in the AASHTO specifications consists of 3 axles spaced at 14ft (4.27m) and 30ft (9.14m), with the largest weight axle load being 32kips (142.3 kN). Because the composite test specimens were 14ft (4.27m) in length, only one axle load is possible within the specimen span and was chosen to be applied at mid-span.

## 4. Results and Discussion

The following sections presents observations and results from the fatigue testing of three composite beam specimens and one non-composite beam specimen. While summaries of averaged slip and separation recordings are provided for comparison in the following section, all individual slip and separation results for Specimens 1, 2, and 3 are provided in Appendix B.

### 4.1. *Observations from Fatigue Testing*

Results from fatigue testing suggest that stud demands estimated by the AASHTO provisions are conservative. All composite specimens tested (both uniform and clustered stud configurations) survived over 4,500,000 fatigue cycles at an applied stress range of 9.8 ksi (67.6 MPa) while maintaining full composite action and experiencing negligible increases in slab slip. Figure 8 shows the progression of slab slip for Specimens 1, 2, and 3, with negligible change in slab slip noticed for the composite specimens over the entire 4,500,000 cycles of loading (see Appendix B for individual slip measurement progressions). Comparing measured slab slip values between Specimen 1 having a uniform stud spacing and Specimen 3 having clustered stud spacing, indicates more slip within the cluster gap region of Specimen 3 (compare Figure 8(a) and Figure 8(c)). The observed increase in gap region slip for the clustered stud specimen is likely due to decreased slab-to-flange friction, as developed tension within the studs of the uniform configuration (Figure 8(a)) provide some normal force between the concrete slab and steel flange during flexural deformations. Not surprisingly, the non-composite specimen (Specimen 2) experienced the largest slab slip on only one side of

the applied load, ranging in value between 0.009 inches and 0.011 inches (0.23mm and 0.29mm) over the fatigue cycles. While the negligible increase in slip over the fatigue cycles indicates a lack of fatigue damage within the studs, observed slab slip during the initial fatigue cycles indicates that the chosen fatigue load level was sufficient to overcome the concrete-to-steel-flange adhesion formed during casting.

The 4,500,000 cycles applied to all composite specimens exceed the current AASHTO provisions estimate of 1,800,000 cycles for fatigue life at 9.81 ksi (67.6 MPa) by 250% [1]. Fatigue life exceedance of 250% is rather large given that the current AASHTO stud provisions are based on the mean response (50% confidence level) of pushout fatigue test data from the 1960's [16]. With recent experimental research justifying the current AASHTO stud fatigue capacities [3], one possible reason for the excess fatigue life is a reduction in actual stud demands through friction load transfer at the steel-concrete interface (all concrete slabs were cast on a Class A friction surface from the clean mill scale flange). Composite beam analyses performed by Oehlers et al. [17] suggest that even small levels of interface friction may provide enough load transfer to drastically reduce stud demands and increase stud fatigue life.

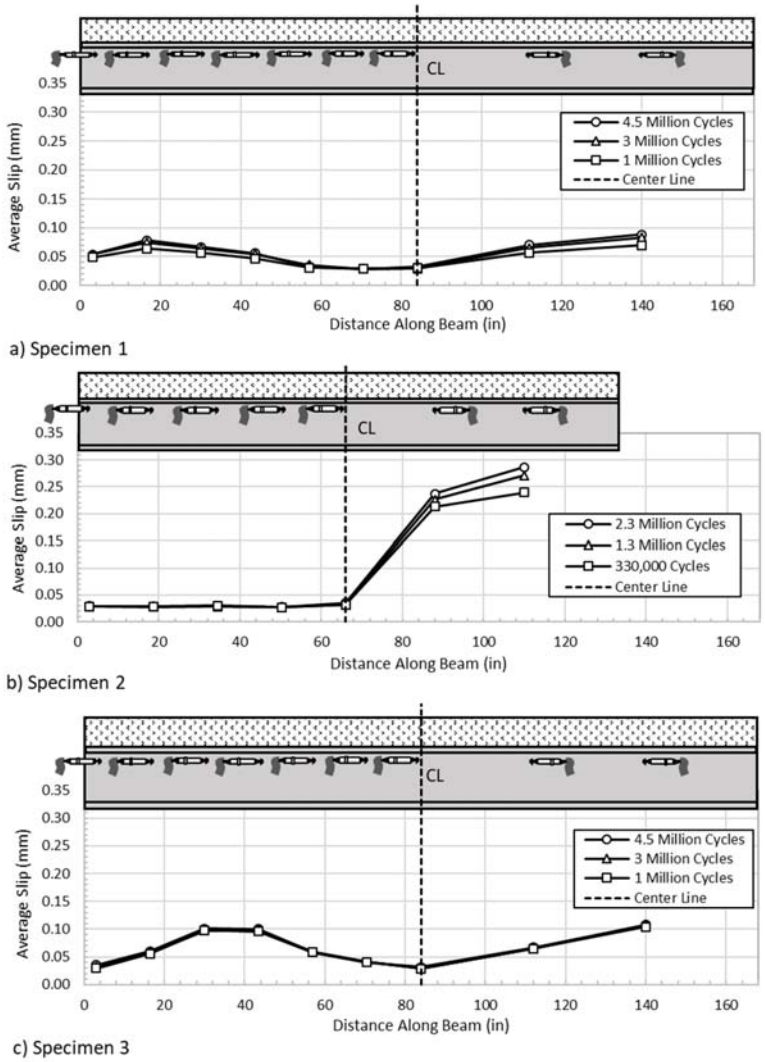


Figure 8. Average slab slip during fatigue loading for a) Specimen 1, b) Specimen 2, and c) Specimen 3

Fatigue test results for Specimen 2 demonstrate the potential for alternative shear transfer mechanisms, as Specimen 2 behaved compositely in the absence of shear studs. Figure 9 shows the upper and lower limit of the measured neutral axis during fatigue testing for Specimen 2 (designed as non-composite) and Specimen 3 (having clustered studs) at the beginning and end of fatigue test. As seen in Figure 9(a), the neutral axis zone for Specimen 2 remains above the non-composite neutral axis location through 2,380,000 cycles prior to ending of the fatigue test. The neutral axis zone for Specimen 3 (Figure 9(b)) remained close to the theoretical short-term composite neutral axis location through all 4,500,000 fatigue cycles.

While the neutral axis measurements, observations of non-composite shear transfer, and survived fatigue cycles all provide evidence that stud demands during fatigue loading are likely lower than those estimated in the AASHTO provisions, direct measurement of stud shear demands are still needed. The following section quantifies the participation of different shear transfer mechanisms and isolates stud demands for comparison with AASHTO estimations.

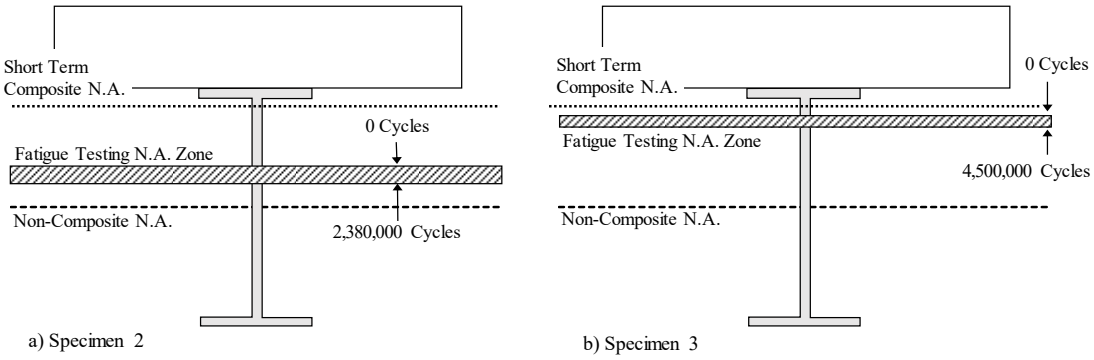


Figure 9. Measured neutral axis locations for Specimen 2 (constructed as non-composite) and Specimen 3 (constructed as composite and having clustered studs) during fatigue loading.

### 4.2. *Stud Shear Demand Calculations from Pressure Gauge Measurements*

Results from the stud pressure gauge measurements indicate that studs only experience concrete contact pressure near the stud-to-flange weld under service-level loadings. Pressure distributions measured from multiple gauges placed along the stud height indicate negligible contact pressure at all locations other than at the shear stud base, within one inch (25.4mm) of the stud-to-flange weld (see Figure 10). Recent analytical investigations have indicated similar findings [18]; however, an accurate understanding of the vertical stud pressure distribution is important for calculating resulting stud demands from the elasticity equations presented earlier. Although pressure readings taken at one inch above the stud base were near zero, to be conservative in estimating stud demands a uniform pressure distribution from the stud base pressure reading was assumed. The conservative nature of this assumption will be checked in a calibration/validation experiment discussed later in Section 5 *Stud Pressure Gauge Measurement Validation*.

Figure 11 shows the calculated stud shear stress, based on the measured peak contact pressure and pressure distribution assuming uniform pressure within the first 1-inch (25.4mm). Note in Figure 11(a) and Figure 11(b) that the calculated shear stress from stud pressure measurements of Specimen 1 and Specimen 3 is lower than the estimated shear stress of 9.8ksi

(67.6 MPa) provided by the AASHTO provisions. Also note that for Specimen 1 and Specimen 3 the concrete slab was cast on top of the cleaned mill-scale steel surface (a Class A friction surface). The average stud shear stress for Specimen 1 and Specimen 3 are 3.21ksi and 3.28ksi (22.1MPa and 22.6MPa) respectively (nearly 66% lower than suggested by the AASHTO provisions). Specimen 4 (see Figure 11(c)), having reduced friction at the steel-concrete interface from the PTFE sheeting noticed a significant increase in shear stress (to 8.9ksi (61.4MPa) on average) which is closer to the calculated value using the AASHTO provisions which neglect friction effects (9.8ksi, 67.5MPa).

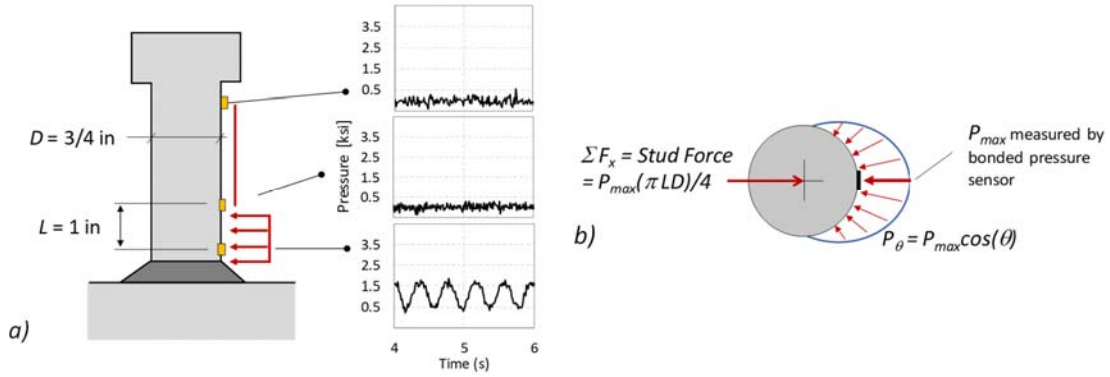


Figure 10. Measured contact pressure distribution along stud height in Specimen 3.

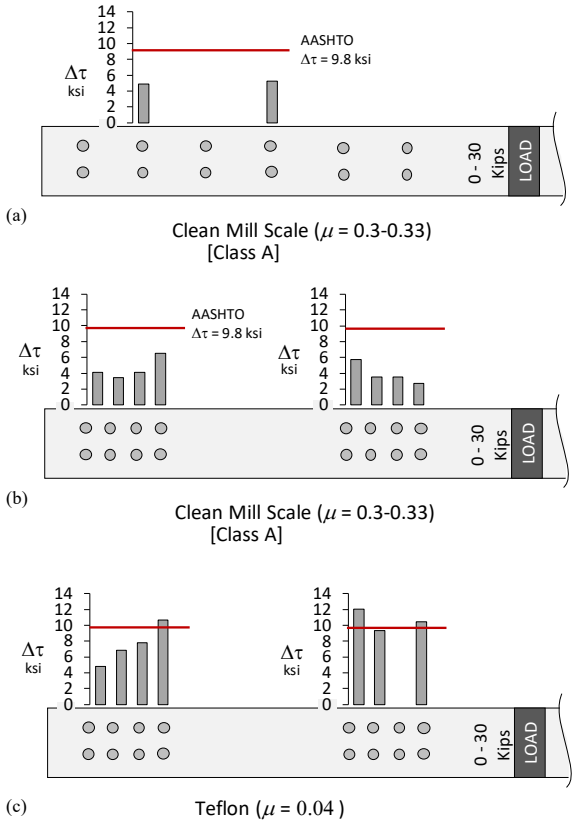


Figure 11. Calculated peak stud shear demands from maximum recorded pressure gauge measurements, a) Specimen 1 with clean mill scale flange surface, b) Specimen 3 with clean mill scale flange surface, and c) Specimen 4 having PTFE sheeting between the flange and concrete slab.

### 4.3. *Effect of Clustering and Flange Surface Friction on Stud Demands*

Comparing stud pressure measurements between Specimen 1 (having uniform studs) and Specimen 3 (having clustered studs) indicates higher demands within the exterior rows of clustered shear studs, somewhat confirming the analytical findings of [2] which suggest increased stud demands within the outer cluster row during moving truck loading. Figure 12 and Figure 13 show examples of the recorded stud pressure measurement variation from cyclic loading at each pressure gauge location for Specimen 1 and Specimen 3 respectively. In Figure 12, the uniformly spaced shear studs experience uniform pressure distributions, as would be expected from a constant shear stress induced by 3-point bending. The exterior studs of the clustered configurations (denoted as S4 and S5 in Figure 13) experience a maximum pressure in the range of 4-5 ksi (27.6-34.5MPa) while the interior stud locations experienced average maximum pressures near 2.8 ksi (19.3MPa). Comparing peak pressure readings between Specimen 1 and Specimen 3 indicates that studs located in the outer rows of the clustered configurations experience similar demands (on average) as studs in the uniformly spaced configurations.

Note in Figure 13 however, that the exterior stud closest to the applied loading measured the lowest stud contact pressure (counter to the findings in [2]). This unexpected result is likely due to the increased friction force between the concrete deck and steel flange (due to the increased normal force) providing an alternate shear load path and reducing demands on the first stud. Figure 14 shows the resulting stud pressure measurements for Specimen 4 (having reduced friction through the addition of PTFE sheets between the steel flange and concrete). While both concrete-to-steel adhesion and friction play a role in additional shear transfer, the fatigue load-level chosen was sufficient to overcome the concrete-to-steel adhesion during the initial fatigue cycles (see again slab slip measurements in Figure 8) indicating that observed demand increase from the PTFE separation is likely the result of friction change. Comparing Figure 14 and Figure 13 the reduced flange friction results in a 210% increase in stud pressure demands on average.

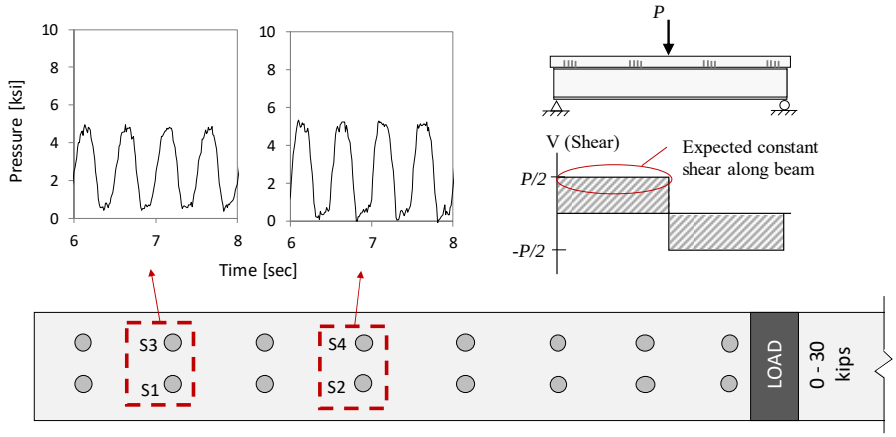


Figure 12. Example of measured pressure distributions on uniformly spaced studs of Specimen 1 having a clean mill scale flange friction surface

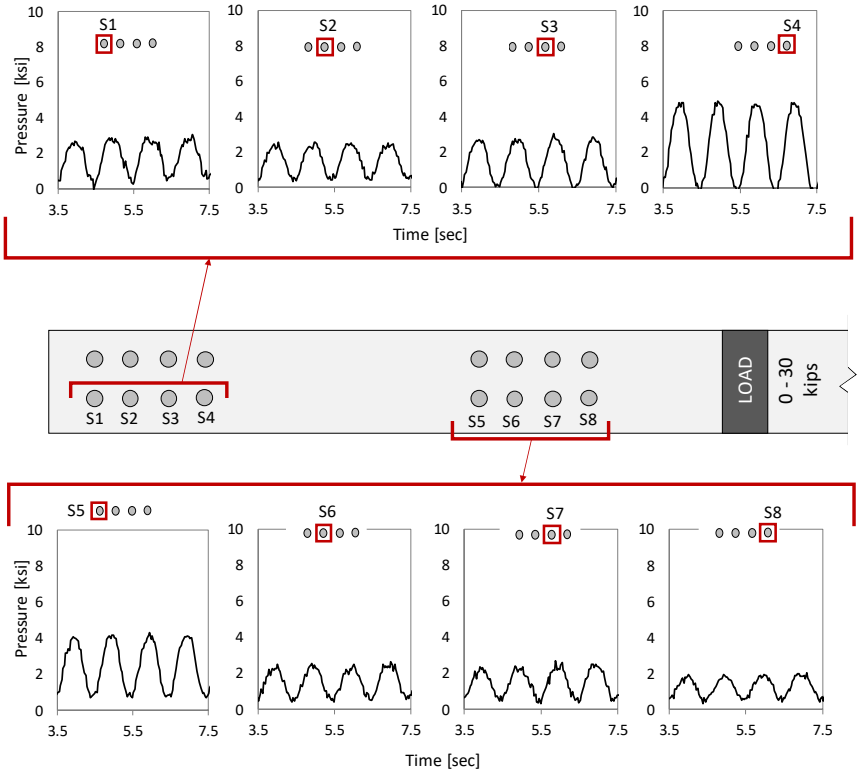


Figure 13. Example of measured pressure distributions on clustered studs of Specimen 3 having a clean mill scale flange friction surface

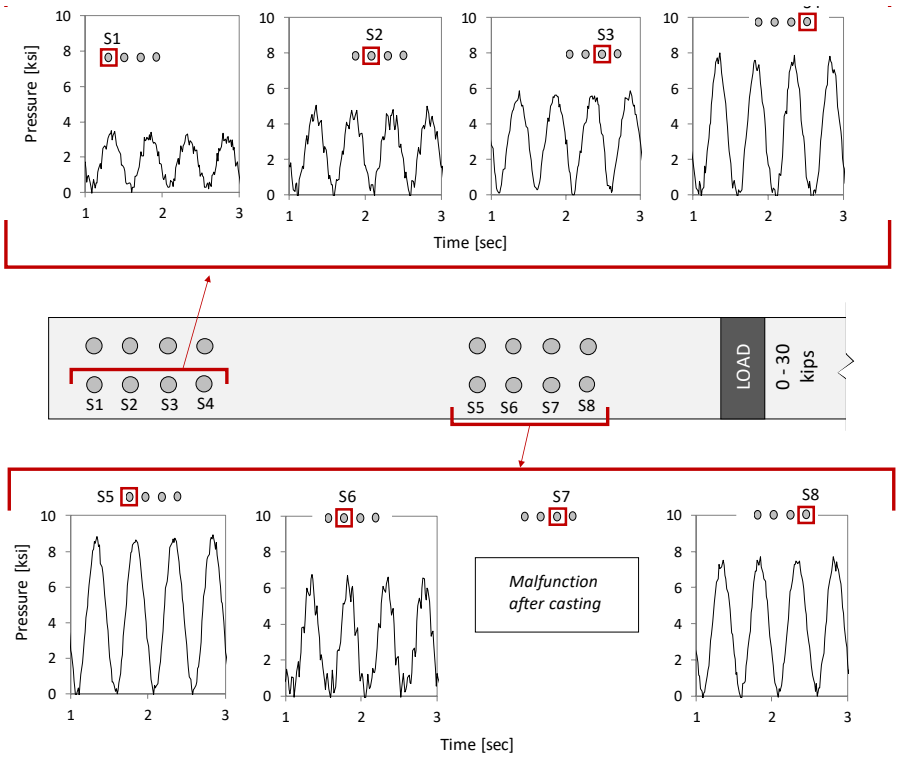


Figure 14. Example of measured pressure distributions on clustered studs of Specimen 4 having PTFE sheeting between the steel flange and concrete slab.

### 4.4. *Implications for Composite Beam Fatigue Design*

In the current AASHTO bridge design provisions, the number of required shear studs is often governed by a fatigue limit state where stud fatigue capacity is balanced with expected stud demands. Stud fatigue demands in the current provisions are calculated from a longitudinal shear flow, $V_{fat}$, based on classical mechanics theory (see Equation 3) and assume no friction or adhesion shear transfer. In the shear flow equation provided in Equation 3, $V$ is the vertical shear force range resulting from passage of the applicable fatigue load, $Q$ is the first area moment of the composite section, and $I$ is the composite section moment of inertia. With the Class A friction surface tested in this study (cleaned mill-scale flange surface), a more than 50% reduction in stud demand was observed. Accounting for flange friction and alternate shear load transfer in design will result in reduced stud demands and fewer shear studs required to meet the fatigue limit state.

Modifying the longitudinal shear flow demand shown in Equation 3 to account for friction load transfer contributions is reasonable and would result in a more balanced design between the fatigue and strength limit states. Equation 4 presents a simple modification to stud fatigue demands based on the measured friction contributions during testing. In Equation 4, $\mu$ would equal 0.5 for a Class A or better flange friction surface or 1 for all other flange friction conditions.

$$V_{fat} = {}^{VQ}/_{I} \qquad \text{(Eq 3)}$$

$$V_{fat} = {}^{\mu VQ}/_{I} \qquad \text{(Eq 4)}$$

To illustrate the implications of the proposed friction modification in Equation 4, consider that each composite beam specimen tested in this study was designed to satisfy the strength limit state only (although tested in fatigue) which required 32 studs at a spacing of 10.8 inches (274mm) to ensure full composite action. To satisfy the current fatigue provisions given by Equation 3, each beam would have required 90 studs at a spacing of 3.8 inches (97mm). Implementing the proposed fatigue demand equation accounting for friction shear transfer (requiring a Class A or better flange friction surface) would result in only 44 studs at a spacing of 7.6 inches (193mm) being required for fatigue, which is more balanced with the stud requirement for strength that performed well under the 4,500,000 fatigue cycles.

## 5. Stud Pressure Gauge Measurement Validation

To verify the concrete-to-stud load transfer mechanism (i.e. the cosinusoidal concrete bearing assumption) and validate the use of the pressure gauges as a stud demand predictor, a validation pushout experiment was conducted. In the validation experiment, load transfer between the concrete slab and steel flange was forced through a single instrumented stud on either side of a pushout specimen as shown in Figure 15. To limit shear transfer through friction or adhesion between the concrete and steel flange, PTFE sheets were placed on a greased steel flange surface prior to concrete casting. Loads were applied to the end of the steel section using a hydraulic loading ram and measured using a 110kip capacity load cell provided in series with the specimen load-path (see again Figure 15). Each stud was instrumented with a single transverse pressure gauge (type PMS40 produced by HBM, inc.) at the base of the stud. All gauges were secured to the stud surface and covered using polymide tape prior to casting.

Comparison between the measured applied load and calculated stud demand from the pressure gauge measurement of the validation test is shown in Figure 16 below. In Figure 16, the peak load calculated from the measured concrete contact pressure at the base of the stud was within 13% on average of the applied demand when a triangular stud pressure distribution over the 1in. (25.4mm) stud integration height was assumed. Given the pressure distribution measurements taken along the stud height in the composite beam tests (see again Figure 10), this triangular distribution assumption (having no pressure at 1in (25.4mm) and the full measured pressure at the base) is reasonable. With the stud force calculations from a triangular pressure distribution matching the applied load in the validation test, the measured stud demands from the composite beam testing appear conservative as they assume a uniform pressure distribution over the entire 1in (25.4mm) integration height. This verifies that the observed 50% reduction in stud demand due to friction at the steel-concrete interface for Class A or better faying surface conditions is likely conservative for service-level loadings.

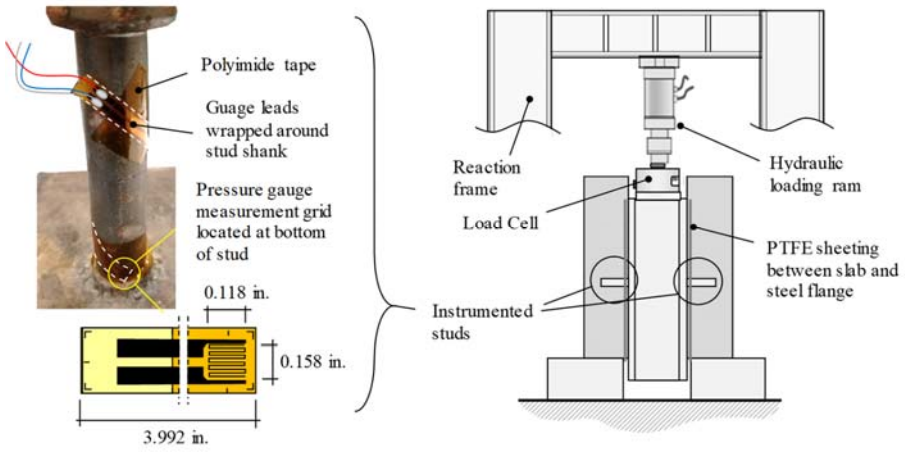


Figure 15. Experimental setup and pressure gauge application for validation test.

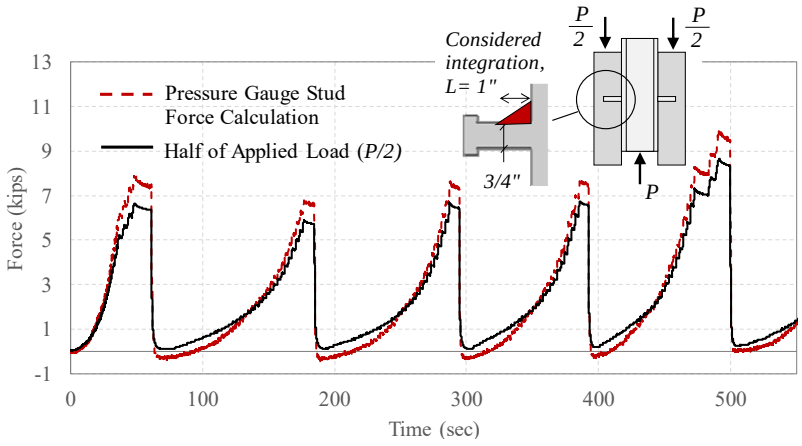


Figure 16. Applied load cycles and resulting stud force measurement assuming a triangular pressure distribution within the first 1in. (25.4mm) of stud height.

## 6. Conclusions

In this study, three large-scale composite beam specimens and one non-composite beam specimen were fatigue tested to investigate shear demands and shear transfer mechanisms.

The three composite specimens were designed based on strength limit state requirements and represent both clustered and uniform stud configurations, as well as different flange surface friction conditions. A stud pressure-measurement approach was developed and applied to the studs of all composite beam specimens to directly measure stud shear demands at the steel-concrete interface. The following are conclusions from the experimental fatigue investigations.

1. Measurements indicate that shear transfer through studs in composite beams subjected to service-level loading occurs within one-inch of the stud-to-flange weld. Pressure distribution measurements along the stud height indicate negligible contact pressure at all locations other than at the base of the shear stud.

2. When a Class A friction surface (or better) is provided by the beam flange, actual shear demands on headed studs are lower than AASHTO estimations due to additional shear transfer from friction. Stud pressure measurements for specimens having a Class A flange friction surface (cleaned mill scale surface) indicated stud demands that were nearly 66% lower than those estimated by the AASHTO provisions which neglect friction effects. When PTFE sheeting was added to reduce friction at the steel-concrete interface, AASHTO stud demand estimations were within 10% of measurements.

3. Current shear stud fatigue provisions are overly conservative for many flange surface conditions and should be modified to account for flange surface friction. All three composite beam specimens (designed to satisfy strength limits) surpassed AASHTO fatigue life estimations by more than 250% (surviving 4,500,000 fatigue cycles at 9.8ksi (67.6 MPa) without loss of composite action or excessive slab slip). A modification to equation 6.10.10.1.2-3 in [1] for estimating stud demands is proposed as $V_{fat} = \mu V_f Q / I$, where $\mu$ equals 0.5 for a Class A or better flange friction surface and $\mu$ equals 1 for all other flange friction conditions.

4. Pressure measurements from the surface of studs in clustered configurations indicate that exterior stud rows are subjected to higher shear demands than interior stud rows, somewhat confirming the findings of [2]. However, studs located in outer rows of the clustered configurations experienced similar shear demands (on average) as studs in the uniformly spaced configurations.

*(Page Intentionally Left Blank)*

## References

[1] AASHTO (2012). "AASHTO LRFD bridge design specifications (6th edition)," *American Association of State Highway and Transportation Officials*, Washington, DC.

[2] B. Ovuoba, and Prinz, G.S. (2018). "Analysis of shear stud fatigue demands in composite bridge girders having varied stud pitch, girder depth, and span length," *J. Bridge Eng.*, 23(11).

[3] B. Ovuoba, and Prinz, G.S. (2016). "Fatigue capacity of headed shear studs in composite bridge girders," *J. Bridge Eng.*, 21(12).

[4] B. Ovuoba, and Prinz, G.S. (2018). "Investigation of residual fatigue life in shear studs of existing composite bridge girders following decades of traffic loading," *Eng. Structures*, 161(2018). pp. 134-145.

[5] J. Provines, and Ocel, J.M. (2014). "Strength and fatigue resistance of shear stud connectors," *National Accelerated Bridge Construction Conference (ABC)*, December, 4-5, Miami, Florida.

[6] M. Sjaarda (2018). "The fatigue behavior of welded and bolted shear connectors in composite highway bridges," *Ph.D. Dissertation*, University of Waterloo, Ontario, Canada.

[7] R. P. Johnson (2000). "Resistance of stud shear connectors to fatigue," *J. Constructional Steel Research*, 56(2000). 101-116.

[8] K.-C. Lee, Abbas, H.H., and Ramey, G.E. (2010). "Review of current AASHTO fatigue design specifications for stud shear connectors," *ASCE Structures Congress Proceedings*, p. 310-321.

[9] D. C. King, Slutter, R.G., and Driscoll, G.C. (1965). "Fatigue strength of 1/2 inch diameter stud shear connectors," *Highway Research Record No. 103*, Publication No. 294.

[10] S. S. Badie, Tadros, M.K., and Girgis, A.F. (2006). "Full-depth, precast-concrete bridge deck panel systems," *NCHRP Report 12-65, Transportation Research Board, National Research Council*.

[11] G. Kwon, Engelhardt, M.D., and Klinger, R.E. (2010). "Behavior of post-installed shear connectors under static and fatigue loading," *J. Constructional Steel Research*, 66(4). pp. 532-541.

[12] P. H. Mans (2001). "Full scale testing of composite plate girder constructed using 70-ksi high performance steel," *M.S. Thesis*, University of Nebraska, Lincoln.

[13] D. Spenlé, and Gourhant, R. (2003). "Guide du calcul en mécanique : maîtriser la performance des systèmes industriels (in French)," *Hachette Technique*.

[14] M. Aublin, Boncompain, R., Boulaton, M., Caron, D., Jeay, E., Lacage, B., and Réa, J. (2005). "Systèmes mécaniques : Théorie et dimensionnement," *Sciences Sup, Dunod.*

[15] AHTD (2014). "Division 800, Section 802: Concrete for structures," *The Arkansas Standard Specification for Highway Construction*.

[16] R. G. Slutter, and Fisher, J.W. (1966). "Fatigue strength of shear connectors " *Highway Research Record No. 147*, Highway Research Board, p. 65-88.

[17] D. J. Oehlers, Rudolf, S., and Yeo, M.F. (2000). "Effect of friction on shear connection in composite bridge beams," *J. Bridge Engineering, ASCE*, 5(2). 91-98.

[18] M. Spremic, Markovic, Z., Dobric, J., Veljkovic, M., and Budevac, D. (2017). "Shear connection with groups of headed studs," *Gradevinar*, 69(2017). 5, pp. 379-386.

## Appendix A. Shear Stud Design for Specimen 1

To evaluate conservancies in the fatigue provisions, all composite beams were designed based on the AASHTO strength limit state (which requires fewer shear studs than the fatigue provisions). The following are design calculations for the required stud pitch (based on strength limits) for the W18×40 composite beam specimens.

**W18 x 40 rolled shape**
**4 in long, 3/4 in diam. Studs**

**Rolled Section Properties**

| | | | | | |
|---|---|---|---|---|---|
| $d$ | = | 17.9 | in | girder depth | |
| $b_f$ | = | 6.02 | in | flange width | |
| $t_f$ | = | 0.525 | in | flange thickness | |
| $d_w$ | = | 16.85 | in | web depth | |
| $t_w$ | = | 0.315 | in | web thickness | |
| $A$ | = | 11.8 | $in^2$ | cross-sectional area | |
| $I$ | = | 612 | $in^4$ | moment of inertia | |
| $S$ | = | 68.4 | $in^3$ | section modulus | |
| $L$ | = | 13.5 | ft | girder length | |
| $L$ | = | 162 | in | girder length | |
| $F_y$ | = | 50 | in | minimum yield strength (A992 steel) | |
| $F_u$ | = | 65 | in | minimum tensile strength (A992 steel) | |

**Shear Stud Properties**

| | | | | | |
|---|---|---|---|---|---|
| $F_y$ | = | 51 | ksi | minimum yield strength (S3L MS stud) | AASHTO 6.4.4 |
| $F_u$ | = | 65 | ksi | minimum tensile strength (S3L MS stud) | AASHTO 6.4.4 |
| $h$ | = | 4 | in | height of stud | |
| $d_s$ | = | 0.75 | in | diameter of body | |
| $d_h$ | = | 1.25 | in | diameter of head | |
| $t_h$ | = | 0.375 | in | head height | |

**Concrete Deck Properties**

| | | | | | |
|---|---|---|---|---|---|
| $f'_c$ | | 3.5 | ksi | assumed concrete strength | |
| $w_c$ | = | 0.150 | kcf | normal weight concrete | |
| $E_c$ | = | 3586.6 | ksi | modulus of elasticity of concrete | AASHTO Eq. 5.4.2.4-1 |
| $t_s$ | = | 6 | in | thickness of concrete slab | |
| $b_s$ | = | 18 | in | effective flange slab width | |

**Check Geometry**

Check Stud Dimensions: AASHTO 6.10.10.1.1

| | | | |
|---|---|---|---|
| h/d | > | 4 | |
| h/d | = | 5.333 | |
| | Check: | 1.333 | OK |

**Calculate Number of Shear Connectors in Cross-Section:** AASHTO 6.10.10.1.3

The flange width is 6 in. Placing the studs a minimum distance of four diameters apart center-to-center with an edge-of-stud to edge-of-flange distance of 1 in allows two studs per row.

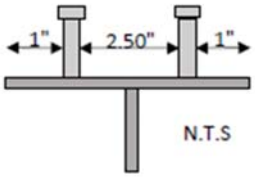


*2 Studs per row

**Calculate Pitch for Strength Limit State** AASHTO 6.10.10.4

$n = P / Q$ AASHTO Eq. 6.10.10.4.1-2

Total Nominal Shear Force

For region from abutment to max positive moment:

$P = \sqrt{(P_p^2 + F_p^2)}$ where $P_p$ = lesser of $P_{1p}$ or $P_{2p}$ AASHTO Eq. 6.10.10.4.2-1

$P_{1p} = 0.85 f'_c b_s t_s$ AASHTO Eq. 6.10.10.4.2-2

$P_{2p} = F_{yw} D t_w + F_{yt} b_{ft} t_{ft} + F_{yc} b_{fc} t_{fc}$ AASHTO Eq. 6.10.10.4.2-3

$F_p = P_p * (L_p / R)$ AASHTO Eq. 6.10.10.4.2-4

*NOTE: $F_p$ taken as zero for straight spans

| | | | | |
|---|---|---|---|---|
| $P_{1p}$ | = | 321.3 | kips | |
| $P_{2p}$ | = | 590 | kips | Simplified to $F_y * A_s$ |
| $P_p$ | = | 321.3 | kips | |
| $F_p$ | = | 0 | kips | |
| P | = | 321.3 | kips | |

*NOTE: Since beam is simply supported, calculations for the region from max positive moment to interior support will not be calculated.

Factored Shear Resistance

$Q_r = \phi_{sc} Q_n$ AASHTO Eq. 6.10.10.4.1-1

$\phi_{sc} = 0.85$ AASHTO 6.5.4.2

$Q_n = 0.5 * A_{sc} * \sqrt{(f'_c E_c)} \leq A_{sc} F_u$ AASHTO Eq. 6.10.10.4.3-1

$A_{sc}$ = cross-sectional area of a stud shear connector ($in^2$)

| | | | | |
|---|---|---|---|---|
| $A_{sc}$ | = | 0.442 | $in^2$ | $\pi d_s^2/4$ |
| $Q_n$ | = | 24.75 | kips | |
| $A_{sc}F_u$ | = | 28.72 | kips | |
| $Q_n$ | = | 24.75 | kips | |
| | | | | |
| $\phi_{sc}$ | = | 0.85 | | |
| $Q_r$ | = | 21.04 | kips | |

Total Number of Shear Connectors

For region from abutment to max positive moment:

| | | | | |
|---|---|---|---|---|
| P | = | 321.3 | kips | |
| Q | = | 21.04 | kips | |
| n | = | 15.3 | studs | n = P / Q |
| $n_{design}$ | = | 16.0 | studs | *round up to nearest even number |

*Therefore each half of the beam must have 16 studs. Total beam will have 32 studs

Pitch of studs

$$p \leq \frac{L * 2 \frac{studs}{row}}{2(n-1)}$$

p = 10.80 in/row

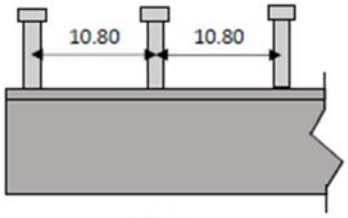


N.T.S

2 studs per row, 16 total per half

*(Page Intentionally Left Blank)*

## Appendix B. Individual Slab Slip and Separation Measurements

The following figures present the individual slab slip and separation progression measurements for Specimens 1, 2, and 3 during the fatigue loading cycles.

### *Specimen 1 (Uniform Stud Spacing)*

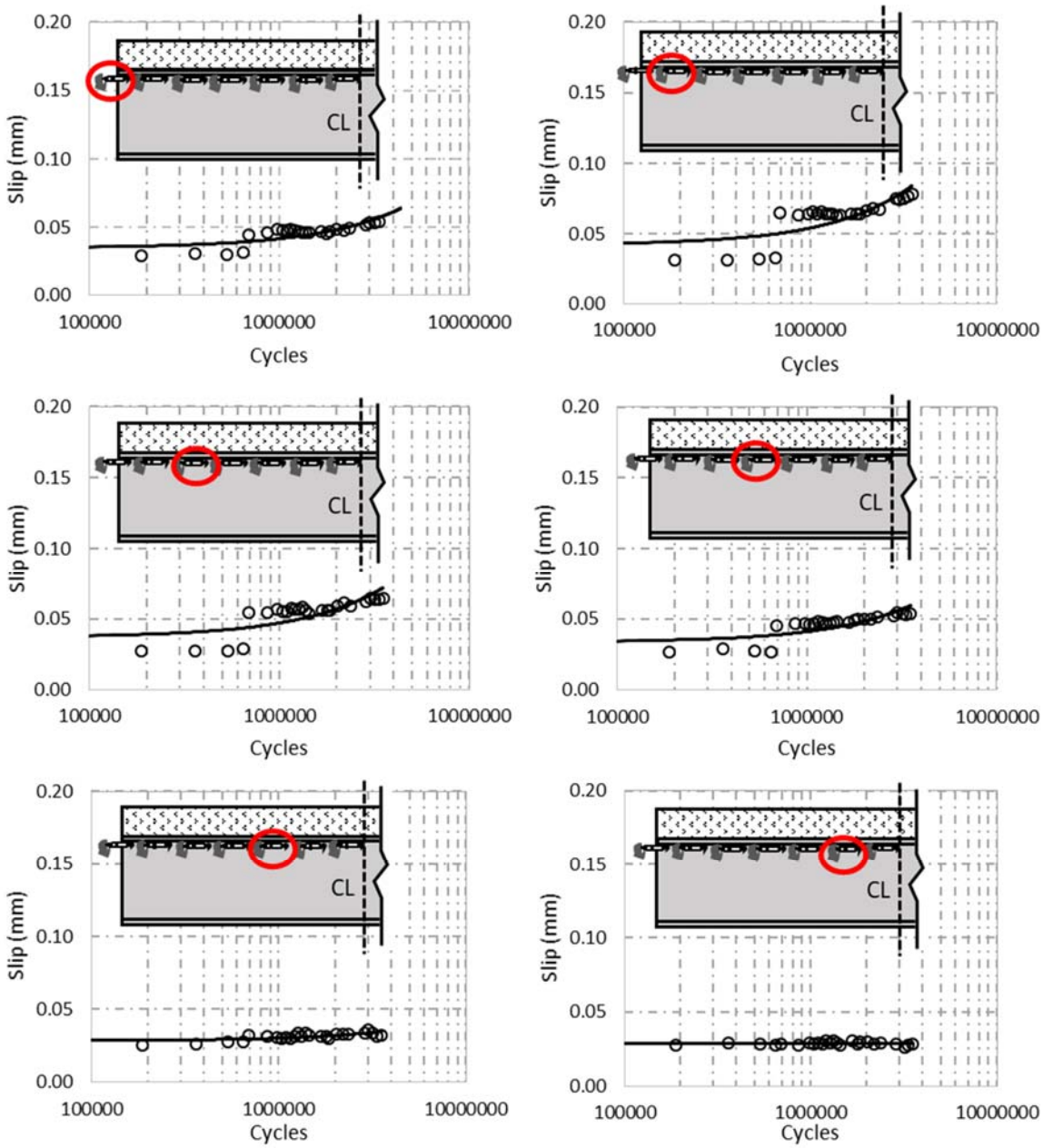

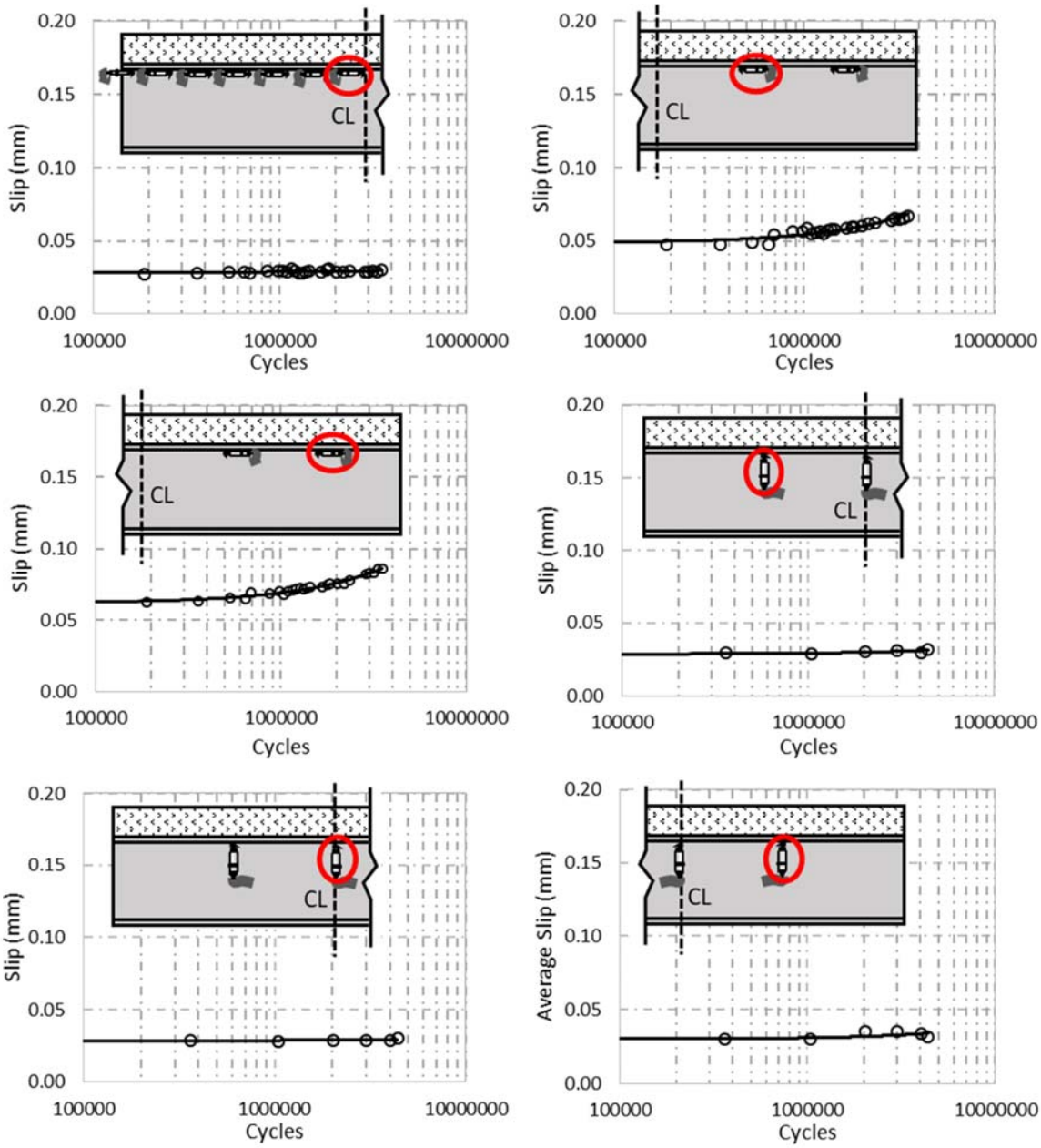
0.20
0.15
0.10
0.05
0.00
Slip (mm)
CL
100000
1000000
10000000
Cycles
0.20
0.15
0.10
0.05
0.00
Slip (mm)
CL
100000
1000000
10000000
Cycles
0.20
0.15
0.10
0.05
0.00
Slip (mm)
CL
100000
1000000
10000000
Cycles
0.20
0.15
0.10
0.05
0.00
Slip (mm)
CL
100000
1000000
10000000
Cycles
0.20
0.15
0.10
0.05
0.00
Slip (mm)
CL
100000
1000000
10000000
Cycles
0.20
0.15
0.10
0.05
0.00
Average Slip (mm)
CL
100000
1000000
10000000
Cycles

***Specimen 2 (Non-Composite)***

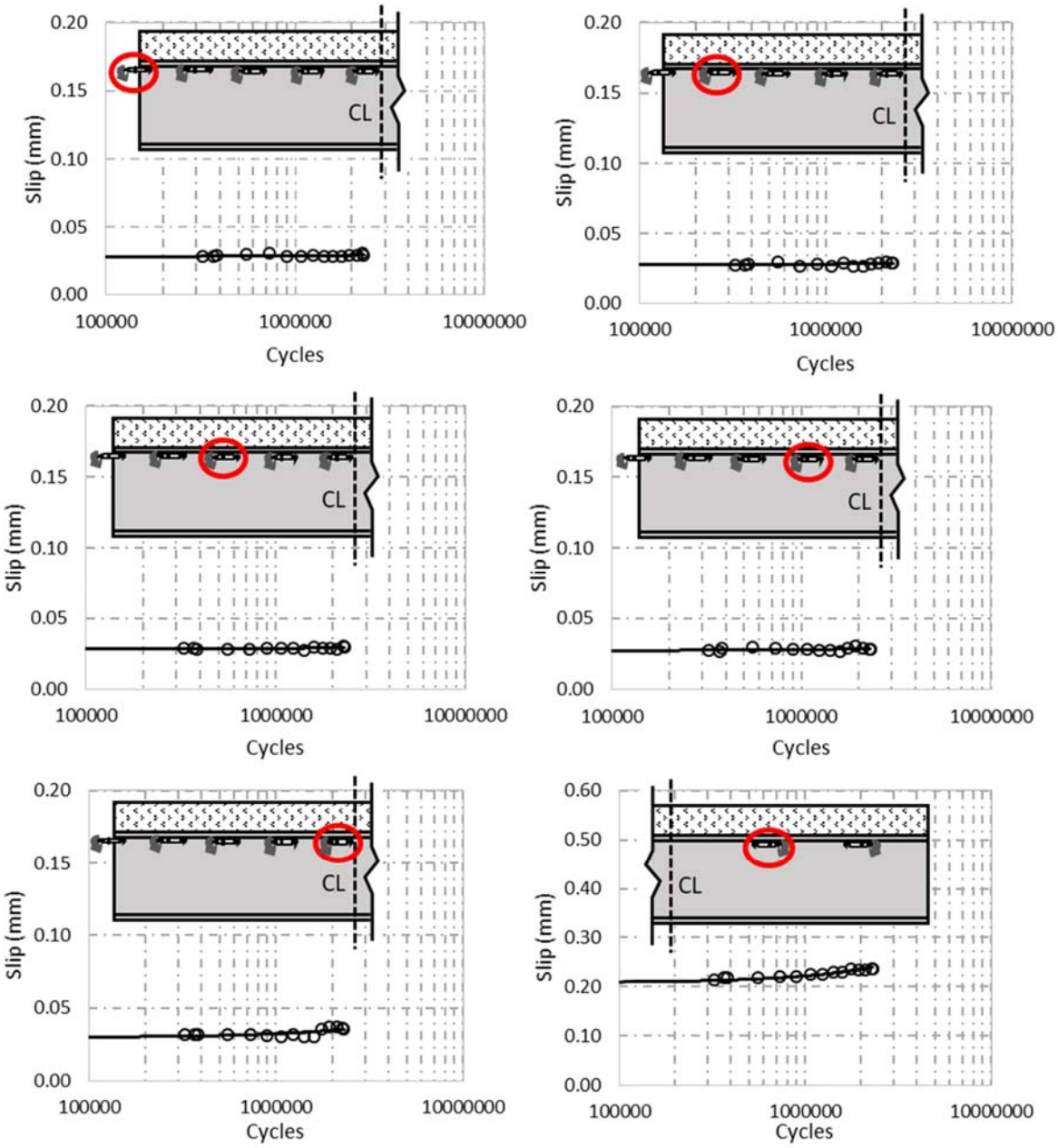

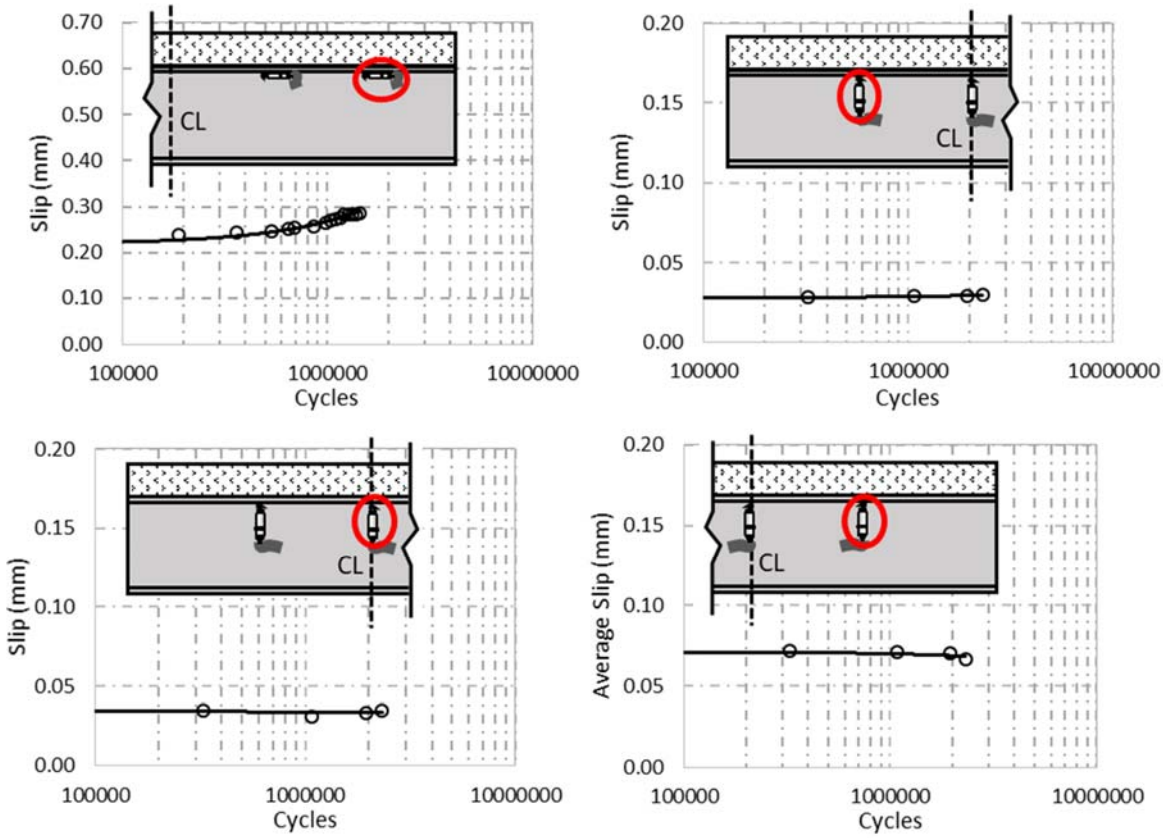
0.70
0.60
0.50
0.40
0.30
0.20
0.10
0.00
Slip (mm)
CL
100000
1000000
10000000
Cycles
0.20
0.15
0.10
0.05
0.00
Slip (mm)
CL
100000
1000000
10000000
Cycles
0.20
0.15
0.10
0.05
0.00
Slip (mm)
CL
100000
1000000
10000000
Cycles
0.20
0.15
0.10
0.05
0.00
Average Slip (mm)
CL
100000
1000000
10000000
Cycles

### *Specimen 3 (Clustered Stud Configuration)*

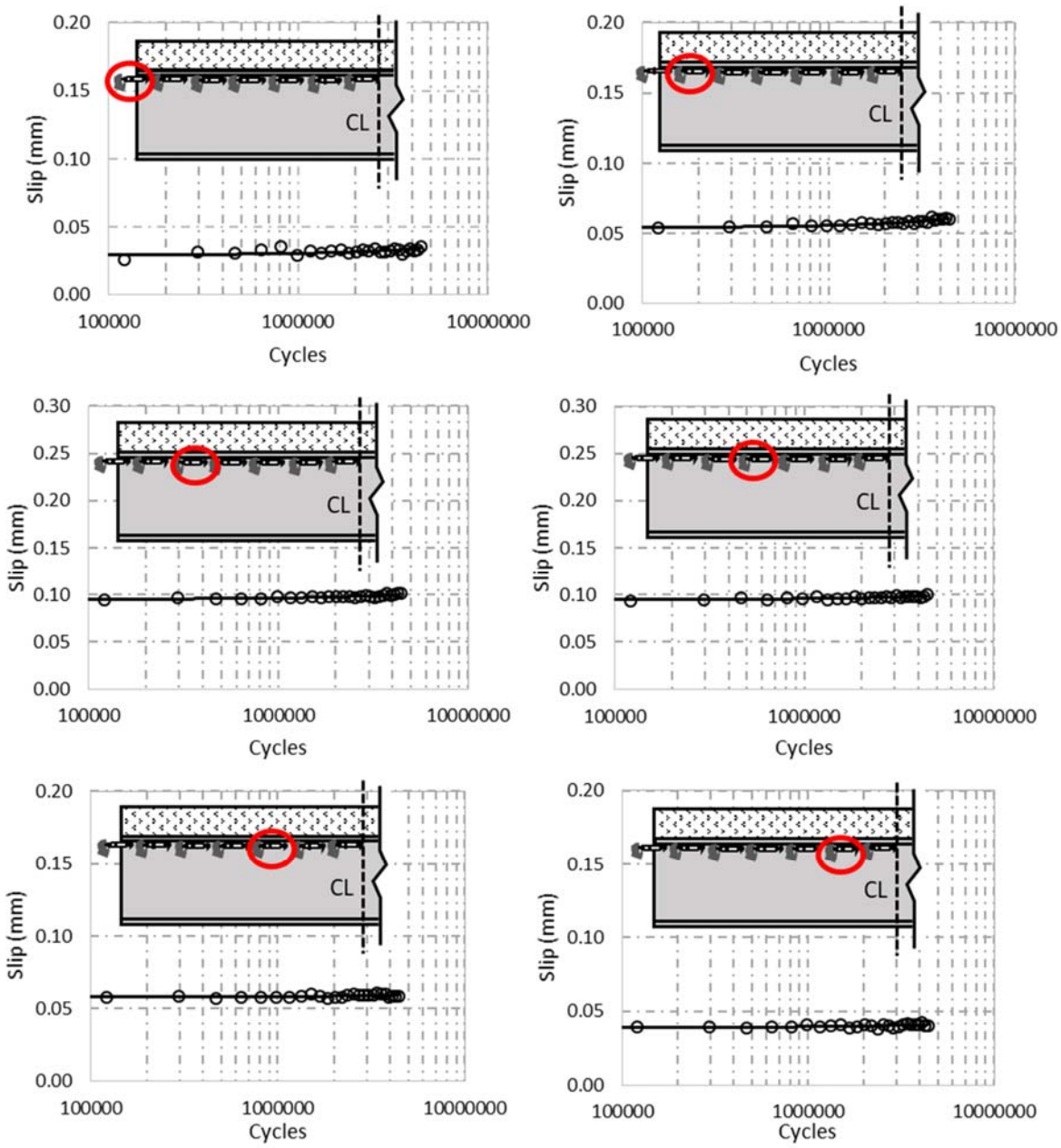

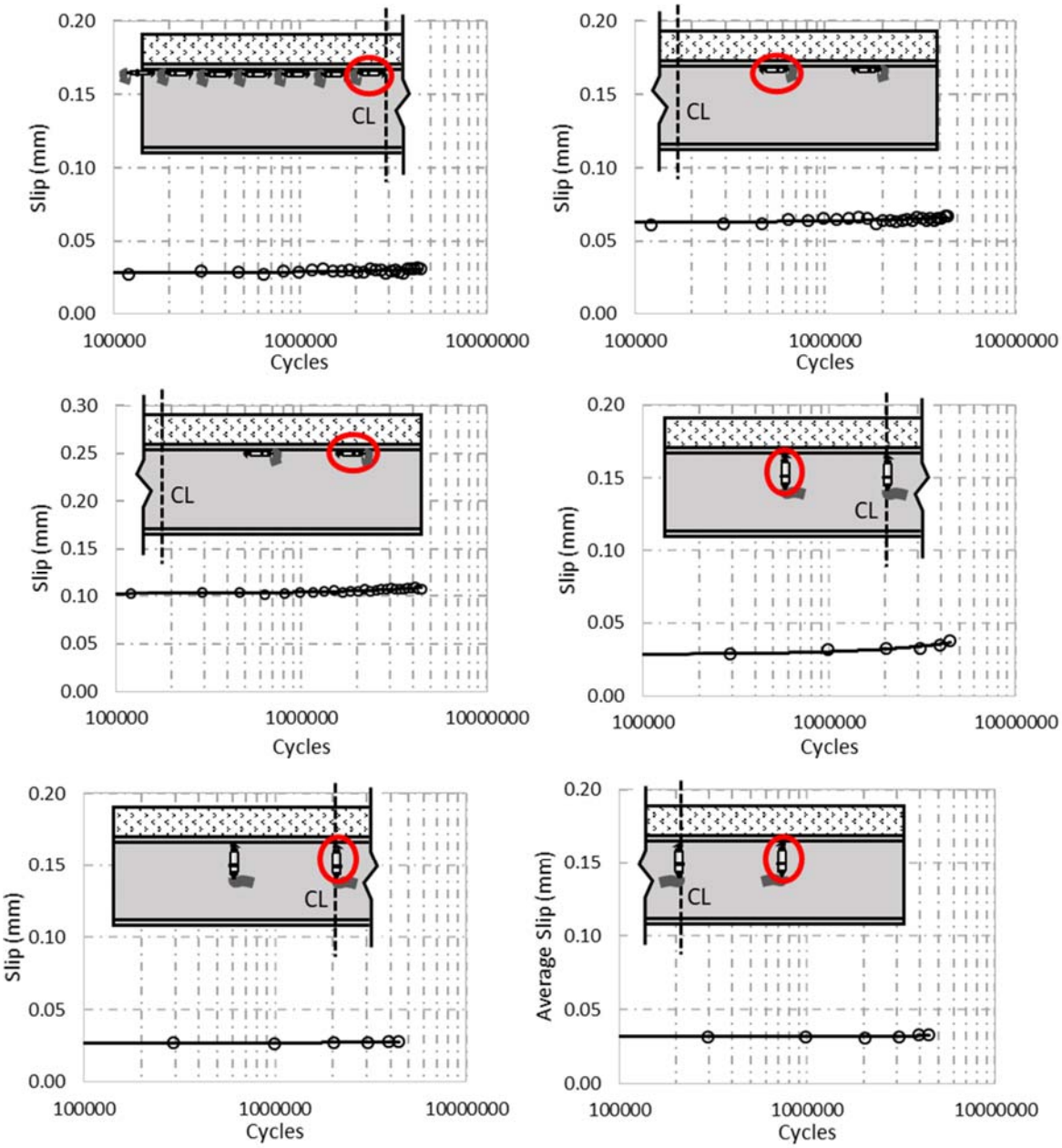
Slip (mm)
Average Slip (mm)
Cycles
CL
100000
1000000
10000000
0.00
0.05
0.10
0.15
0.20
0.25
0.30